Modulation of Synaptic Plasticity and Memory by Reelin Involves Differential Splicing of the Lipoprotein Receptor Apoer2

Uwe Beffert,[1] Edwin J. Weeber,[4] Andre Durudas,[1]
Shenfeng Qiu,[4] Irene Masiulis,[1] J. David Sweatt,[5]
Wei-Ping Li,[2] Giselind Adelmann,[6]
Michael Frotscher,[6,7] Robert E. Hammer,[3]
and Joachim Herz[1,7,*]
[1]Department of Molecular Genetics
[2]Department of Cell Biology
[3]Department of Biochemistry
University of Texas Southwestern Medical Center
Dallas, Texas 75390
[4]Department of Molecular Physiology and Biophysics
Vanderbilt University
Nashville, Tennessee 37232
[5]Division of Neuroscience
Baylor College of Medicine
Houston, Texas 77030
[6]Institut für Anatomie und Zellbiologie
[7]Zentrum für Neurowissenschaften
Albert-Ludwigs-Universität Freiburg
Albertstr. 17
D-79104 Freiburg
Germany

Summary

Apolipoprotein E receptor 2 (Apoer2), a member of the LDL receptor gene family, and its ligand Reelin control neuronal migration during brain development. Apoer2 is also essential for induction of long-term potentiation (LTP) in the adult brain. Here we show that Apoer2 is present in the postsynaptic densities of excitatory synapses where it forms a functional complex with NMDA receptors. Reelin signaling through Apoer2 markedly enhances LTP through a mechanism that requires the presence of amino acids encoded by an exon in the intracellular domain of Apoer2. This exon is alternatively spliced in an activity-dependent manner and is required for Reelin-induced tyrosine phosphorylation of NMDA receptor subunits. Mice constitutively lacking the exon perform poorly in learning and memory tasks. Thus, alternative splicing of Apoer2, a novel component of the NMDA receptor complex, controls the modulation of NMDA receptor activity, synaptic neurotransmission, and memory by Reelin.

Introduction

Cells use receptors at the plasma membrane to interact and communicate with the extracellular environment and with each other. This frequently involves the uptake of macromolecules through endocytosis, or coupling of the receptors to intracellular signaling pathways. Receptor specificity, intracellular trafficking, and signaling can be modulated by alternative and differential splicing, a mechanism thought to contribute to the increased functional complexity of the mammalian proteome (Black and Grabowski, 2003; Grabowski and Black, 2001).

The LDL receptor gene family constitutes a class of structurally closely related, yet remarkably versatile, multifunctional endocytic cell surface receptors that regulate a wide range of cellular signaling pathways (Strickland et al., 2002). Some members of this ancient family of lipoprotein receptors are also subject to extensive alternative splicing of as yet unknown biological significance. A common ligand for all members of the gene family is apolipoprotein E (ApoE), a polymorphic gene strongly associated with late-onset Alzheimer's disease. Some members of the family serve primarily as transporters for cholesterol-carrying lipoproteins. Others, such as the very low density lipoprotein receptor (Vldlr) and the ApoE receptor-2 (Apoer2, also known as Lrp8), function in a partly overlapping manner during brain development, where they control the ordered formation of cortical layers (Trommsdorff et al., 1999) through a mechanism that activates signaling pathways rather than cargo transport. Both Apoer2 and Vldlr serve as receptors for Reelin (D'Arcangelo et al., 1999; Hiesberger et al., 1999; Jossin et al., 2004), a large signaling molecule that is produced by Cajal-Retzius neurons at the surface of the developing neocortex. Reelin-induced receptor clustering (Strasser et al., 2004) results in tyrosine phosphorylation of Disabled-1 (Dab1) (Howell et al., 1999a), an adaptor protein that interacts with conserved NPxY motifs in the cytoplasmic domains of Vldlr and Apoer2 (Howell et al., 1999b; Trommsdorff et al., 1998, 1999).

Dab1 tyrosine phosphorylation is essential for the propagation of the Reelin signal within the migrating cell (Howell et al., 2000), where it amplifies the activity of nonreceptor tyrosine kinases of the Src family (Arnaud et al., 2003; Bock and Herz, 2003). This results in the recruitment and activation of PI3 kinase by phosphorylated Dab1 (Bock et al., 2003) and the regulation of additional cytosolic kinases that modulate the phosphorylation of target proteins, such as the microtubule-associated protein tau (Beffert et al., 2002), which is abnormally phosphorylated in the brains of patients suffering from Alzheimer's disease.

Reelin is also a highly conserved molecule that is present in all vertebrates studied to date (Tissir and Goffinet, 2003). With the end of the neuronal migration period, Reelin expression by Cajal-Retzius neurons subsides and is replaced by expression from a subset of GABAergic interneurons interspersed throughout the neocortex and hippocampus (Alcantara et al., 1998; Drakew et al., 1998), a class of inhibitory neurons that control excitatory neuronal networks and thus regulate synaptic transmission and plasticity. On an evolutionary time scale, the LDL receptor gene family made its first appearance in primitive multicellular organisms such as *C. elegans*, and its structural organization has remained essentially unchanged. With the appearance of the mammalian kingdom, a new exon that is not present in birds was added to the cytoplasmic domain of Apoer2

*Correspondence: joachim.herz@utsouthwestern.edu

(Brandes et al., 1997). This exon is differentially spliced in the brain, and the stretch of amino acids encoded by this exon was found to interact with scaffolding proteins that function in *trans*-synaptic and intracellular signaling. Taken together, these observations argue for a distinct function for Reelin in the adult brain that is different from its role in regulating neuronal migration during development.

We have recently reported a potent physiological function for Reelin and ApoE receptors in modulating long-term potentiation and learning (Weeber et al., 2002), demonstrating a novel and larger role for this signaling pathway in the regulation of neurotransmission. Since alternative splicing frequently occurs in proteins involved in neurotransmission, we wanted to explore the role of the alternatively spliced intracellular domain (ICD) of Apoer2 in transmitting the Reelin signal in the adult brain. In this study, we used a knockin approach in mice to demonstrate that Reelin-mediated enhancement of long-term potentiation depends upon the presence of the 59 amino acids that are encoded by the alternatively spliced exon 19 (ex19). This exon is also necessary for the stimulation of tyrosine phosphorylation of NMDA receptor (NR2) subunits in hippocampal slices in response to Reelin. The splicing is regulated in an activity-dependent manner, and mice expressing mutant Apoer2 receptors lacking ex19 are severely deficient in learning and memory, processes for which NMDA receptors are essential. Apoer2 and Dab1 are present in the postsynaptic density where Apoer2 resides in a complex with NMDA receptors. These findings establish a molecular mechanism by which Reelin, in conjunction with regulated alternative splicing of ApoE receptors, regulates synaptic function, learning, and memory in the adult brain.

Results

Generation of Apoer2 Knockin Mutants

The intracellular domain (ICD) of Apoer2 interacts with several cytosolic adaptor and scaffolding proteins, which include Dab1 (Trommsdorff et al., 1999), PSD-95 (Gotthardt et al., 2000), and JIP1 and -2 (Gotthardt et al., 2000; Stockinger et al., 2000). While Dab1 binds tightly through its PTB domain to a short linear sequence stretch containing an NPxY consensus motif (Stolt et al., 2003; Yun et al., 2003), JIP1/2 and PSD-95 interact preferentially with sequences in the alternatively spliced exon 19 in the Apoer2 ICD (Gotthardt et al., 2000; Stockinger et al., 2000). In order to explore the physiological significance of this alternative splicing event, we have used a knockin approach to generate two strains of mice that constitutively lack or express the 59 amino acid insert that is encoded by this exon.

A replacement-type knockin vector was designed as shown in Figure 1A to direct expression from a cDNA cassette that was inserted by homologous recombination into the Apoer2 locus. A schematic that shows both forms of the ICD that either constitutively express the alternatively spliced exon 19 (ex19) or lack it completely (Δex19) is shown in Figure 1B. Mice generated from targeted ES cells were bred to homozygosity and verified by Southern blotting and PCR (Figures 1C and

1D). To remove the neomycin (*neo*) resistance cassette used for ES cell targeting, the mutant animals were also crossed with a deleter strain of mice that express Cre recombinase in their germline. All mice used for subsequent analyses lacked the *neo* cassette.

To verify that all mutant alleles were expressed at normal levels in vivo, neuronal membrane extracts from the indicated mouse strains (Figure 1E) were immunoblotted with three antibodies directed against different epitopes in Apoer2. All receptor forms were detected by antibodies directed either against the extracellular domain (αED) or the carboxyl terminus (αCT). αEX19 is directed against an epitope within exon 19, which is absent in the Δex19 mutant.

Exon 19 Is Not Required for Normal Neuronal Positioning

Apoer2 is critical for normal neuronal positioning in the neocortex and in the hippocampus and, together with the Vldlr, for the development of the cerebellum (Trommsdorff et al., 1999). To evaluate the effect of the absence or presence of the alternatively spliced ICD insert encoded by exon 19, we examined sagittal H&E sections from 3-week-old (P21) mice expressing either of the two ICD forms (Figure 2A). Wild-type (panel a) and Apoer2 (*Apoer2$^{-/-}$*) knockout mice (panel b) served as controls. As reported earlier (Trommsdorff et al., 1999), Apoer2 knockouts have marked neuronal positioning defects throughout the CA1–CA3 regions and the dentate (DG). By contrast, the hippocampus of mice constitutively expressing (ex19, panel c) or lacking exon 19 (Δex19 panel d) were indistinguishable from the wild-type. The lamination of the neocortex and the foliation and Purkinje cell positioning in the cerebellum were also unaffected (data not shown). Thus, absence of the ICD insert alone does not affect neuronal positioning in the mammalian brain.

Tyrosine Kinase Activation Does Not Require the Alternatively Spliced Insert

Reelin binding to Apoer2 and Vldlr activates a kinase cascade that involves Src family members, PI3 kinase, and the serine/threonine kinases Akt and Gsk3 (Arnaud et al., 2003; Beffert et al., 2002; Bock and Herz, 2003; Bock et al., 2003). We assessed the ability of Reelin to stimulate Dab1 and Akt phosphorylation in cultured embryonic forebrain neurons from each of the Apoer2 ICD mutants as described previously (Beffert et al., 2002). We performed this assay in the absence of functional Vldlr, since either Apoer2 or Vldlr alone are sufficient to induce Dab1 tyrosine phosphorylation in vitro (Beffert et al., 2002), although both receptors are necessary for normal neuronal migration in vivo (Trommsdorff et al., 1999).

As shown in Figure 2B, phosphorylation of Dab1 and Akt in neurons was dependent upon Reelin (lanes 1 and 2) and did not occur in neurons lacking both receptors (lanes 3 and 4). The presence (lanes 5 and 6) or absence (lanes 7 and 8) of exon 19 did not affect the ability of Reelin to induce Dab1 or Akt phosphorylation, indicating that the insert encoded by exon 19 is not required for the initial activation and intracellular propagation of the Reelin signal. We thus decided to explore whether it might be required for the coupling of the sig-
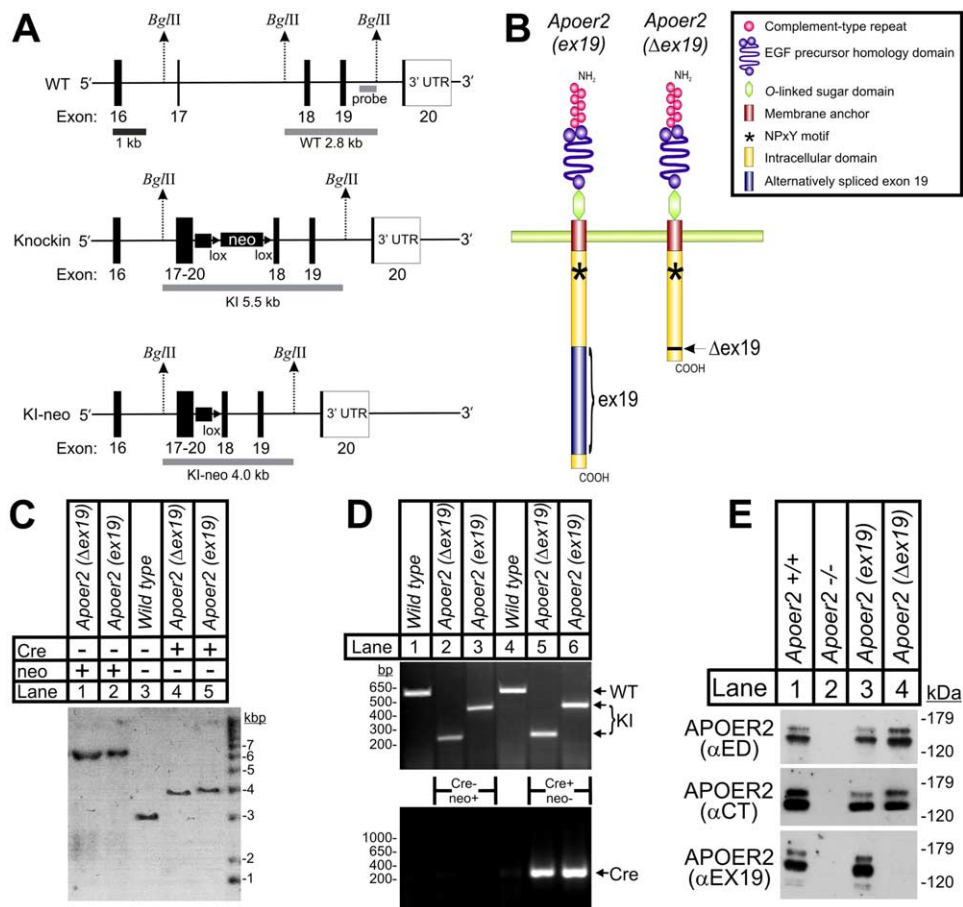
Figure 1. Generation of *Apoer2* ICD Knockin Mice

(A) Wild-type genomic and mutated loci before and after excision of neomycin (*neo*) resistance gene with Cre recombinase. The top panel shows the wild-type *Apoer2* locus and location of exons 16 through 20, including introns. The Southern probe used for genotyping is located between exons 19 and 20. Upward arrows indicate BglII sites used to generate fragments for Southern genotyping. The middle panel illustrates the mutated allele containing a cDNA cassette that includes exons 17 through 20 and the indicated mutations to the ICD. The *neo* cassette is flanked by *loxP* sites (indicated by triangles). The lower panel shows the mutated *Apoer2* locus following excision of the *neo* with Cre recombinase. (Drawn to scale.)

(B) Schematic illustration of the two receptor isoforms. *Apoer2* (*ex19*) and *Apoer2* (*Δex19*) represent wild-type splice variants of exon 19 (not drawn to scale).

(C) Southern blot of BglII-digested genomic DNA using the probe indicated in Panel (A). Wild-type band, 2.8 kb (lane 3); mutated allele containing the *neo* cassette, 5.5 kb (lanes 1 and 2); mutated allele without the *neo* cassette, 4.0 kb (lanes 4 and 5). Both *Apoer2* (*Δex19*) alleles (lanes 1 and 4) are 177 bp shorter than the *Apoer2* (*ex19*) alleles (lanes 2 and 5).

(D) PCR genotyping of knockin mice. Wild-type product, 603 bp (lanes 1 and 4); Apoer2 (ex19), 451 bp product (lanes 3 and 6); *Apoer2* (*Δex19*), 274 bp product (lanes 2 and 5). Bottom panel, 400 bp Cre recombinase PCR band.

(E) Detection of Apoer2 ICD mutant proteins with domain-specific antibodies. Western blotting of primary embryonic cortical mouse neurons with anti-Apoer2 antibodies αED (against the extracellular domain), αCT (against the wild-type carboxyl terminus), and αEX19 (against exon 19) reveals normal expression from the mutant alleles.

nal to other compartments of the neuronal signal transmission machinery, such as ion conduction channels in the synapse.

Exon 19 Is Required for Reelin-Enhanced LTP

We have shown earlier that Apoer2 is involved in hippocampal LTP in area CA1, but is not involved in the mechanisms underlying basal synaptic transmission (Weeber et al., 2002). To further explore the role of Apoer2 signaling in the adult hippocampus, we probed the well-defined Schaffer collateral synapses for altered synaptic function and synaptic plasticity in hippocampal slices from our ICD mutants. As shown in

Figure 2A, neuronal positioning and anatomy of the hippocampus are unaltered in these mice and indistinguishable from wild-type.

Overall synaptic transmission was determined from the population excitatory postsynaptic potentials (pEPSPs) of field recordings from hippocampal area CA1 synapses and evaluated by determining the amplitude of the evoked fiber volley versus the slope of pEPSP at increasing stimulus intensities (Figure 3A). Linear regression analysis revealed no significant difference in the first differential for any of the mutant animals (*Apoer2* [*ex19*], slope = 2.99 ± 0.24; *Apoer2* [*Δex19*], slope = 2.02 ± 0.29). This suggests that the overall con-
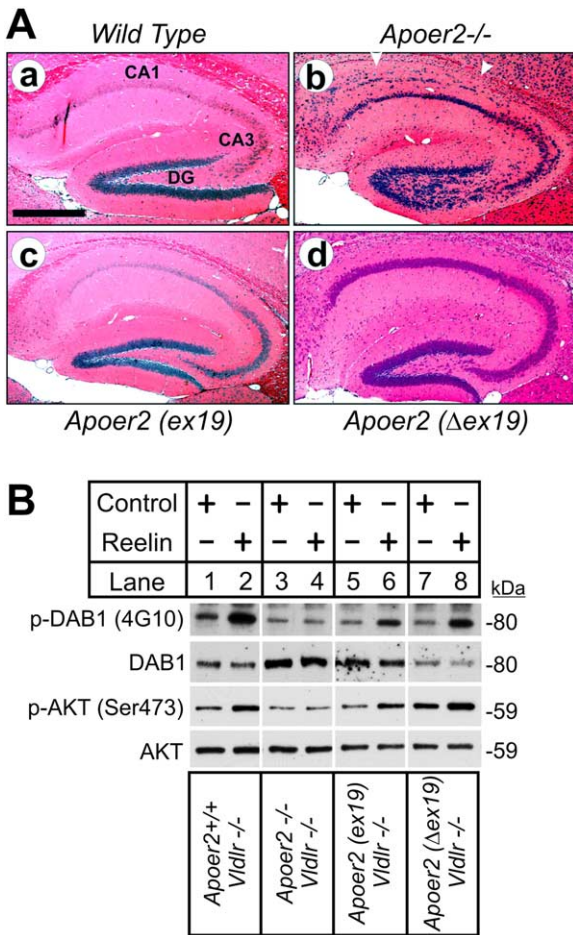
A

Wild Type   *Apoer2-/-*

a   CA1   CA3   DG

b

c

d

Apoer2 (ex19)   *Apoer2 (Δex19)*

B

Control	+	−	+	−	+	−	+	−	
Reelin	−	+	−	+	−	+	−	+	
Lane	1	2	3	4	5	6	7	8	kDa

p-DAB1 (4G10) — -80
DAB1 — -80
p-AKT (Ser473) — -59
AKT — -59

Apoer2+/+ / Vldlr -/-   Apoer2 -/- / Vldlr -/-   Apoer2 (ex19) / Vldlr -/-   Apoer2 (Δex19) / Vldlr -/-

Figure 2. Normal Neuronal Positioning and Reelin Signaling in Apoer2 ICD Mutants

(A) Histoanatomy of hippocampus of *Apoer2* ICD Mutants. Hematoxylin and eosin staining of sagittal brain sections from P21 mouse cerebral cortex from (Aa) wild-type, (Ab) *Apoer2*$^{-/-}$, (Ac) *Apoer2* (*ex19*), and (Ad) *Apoer2* (*Δex19*). Scale bars in (A) = 500 μm. CA1 and CA3, *Cornu Ammonis* subfields 1 and 3 of the hippocampus; DG, dentate gyrus. Arrows (Ab) indicate split CA1 and neuronal positioning defects in CA3.

(B) Reelin signaling through Dab1 and Akt does not require the exon 19-encoded sequences. Mouse cortical neurons (5 days in vitro) were prepared from E16 embryos from the indicated *Apoer2* and *Vldlr* mutant and control mice and incubated with either control or Reelin containing medium for 20 min. In the absence of *Vldlr*, Reelin induces tyrosine phosphorylation of Dab1 and serine phosphorylation of Akt at residue 473 (lane 2) over control medium (lane 1). In the absence of *Apoer2* and *Vldlr* (lanes 3 and 4), no increase in Dab1 or Akt phosphorylation is seen. Reelin-induced phosphorylation is normal in *Apoer2* (*ex19*);*Vldlr*$^{-/-}$ (lanes 5 and 6) and *Apoer2* (*Δex19*);*Vldlr*$^{-/-}$ (lanes 7 and 8).

nectivity across Schaffer collateral synapses is unaltered in both mutants. Short-term plasticity was evaluated using paired-pulse facilitation and revealed no significant differences in either of the animal groups compared to each other or compared to wild-type control mice, with the exception of the 50 ms interpulse interval, which was marginally reduced in the *Apoer2* (*Δex19*) mice (Figure 3B). Thus, we cannot rule out a minor contribution of Apoer2 to presynaptic functions.

Because LTP is impaired in Apoer2-deficient mice, we decided to investigate the role of the ICD on Apoer2- and NMDA receptor-dependent synaptic plasticity. We had previously established that a theta burst stimulation (TBS) protocol most prominently revealed the LTP deficit in Apoer2-deficient mice (Weeber et al., 2002). The degree of potentiation produced with this protocol was similar in all groups (Figure 3C). Thus, no significant differences of synaptic transmission, paired-pulse facilitation, and TBS-induced LTP were seen between wild-type and *Apoer2* (*ex19*) and *Apoer2* (*Δex19*) mice.

We have reported earlier that Reelin increased LTP induction in wild-type hippocampus slices. In addition, this increase in potentiation was dependent upon the presence of Apoer2 (Weeber et al., 2002). We therefore sought to determine the response of LTP to Reelin in our Apoer2 ICD mutants. In response to Reelin, *Apoer2* (*ex19*) mice showed a robust increase in LTP induction (Figure 3D), which was completely abrogated in the neuroanatomically indistinguishable *Apoer2* (*Δex19*) mutant (Figure 3E).

To test whether the enhancement of LTP by Reelin is due, at least in part, to the modulation of NMDA receptors, we determined the effect of Reelin on NMDA receptor potentials in hippocampal slices for each animal group (Figure 3F). We found that Reelin potentiates NMDA receptor-mediated pEPSPs recorded in area CA1 when AMPA receptors are blocked with 6-cyano-7-nitroquinoxaline-2,3-dione (CNQX). Wild-type and *Apoer2* (*ex19*) mice showed a similarly significant increase in NMDA receptor potentials upon Reelin perfusion, which was maintained longer in the *Apoer2* (*ex19*) mutants. By contrast, the *Apoer2* (*Δex19*) mutant showed no elevation of NMDA receptor-dependent potentials above baseline synaptic responses ($F_{[2,300]}$ = 71.2, $p < 0.0001$, ANOVA). Reelin had no effect on AMPA receptor-mediated field potentials (see the Supplemental Data available online).

To verify that the increased NMDAR function seen during our field recording was the direct effect of Reelin acting on postsynaptic neurons, we applied Reelin to synaptically evoked whole-cell NMDAR-mediated EPSCs (NMDA-EPSC) in wt CA1 neurons (voltage clamped at +30 mV) in the presence of the GABA$_A$ receptor blocker picrotoxin (100 μM) and CNQX (10 μM). Reelin increased NMDA-EPSC in seven of eight CA1 pyramidal cells tested (Figures 4A1 and 4B); the increase was seen within 10 min from the start of Reelin application and lasted up to 1 hr. The parallel column fractions from untransfected HEK293 culture medium (Mock) showed no effect on NMDA-EPSC. We further asked whether the Reelin effect was specific to NMDARs by examining isolated AMPAR responses to Reelin. In the presence of 100 μM picrotoxin and 100 μM D(-)-2-amino-5-phosphopentanoic acid (AP-5 or APV), AMPA-EPSC was not changed by a 20 min application of Reelin (Figures 4A2 and 4C).

Taken together, these data indicate that LTP enhancement by Reelin involves a molecular mechanism that is dependent upon the alternatively spliced exon 19. In addition, this mechanism involves, at least in part, the modulation of NMDA receptor functions.
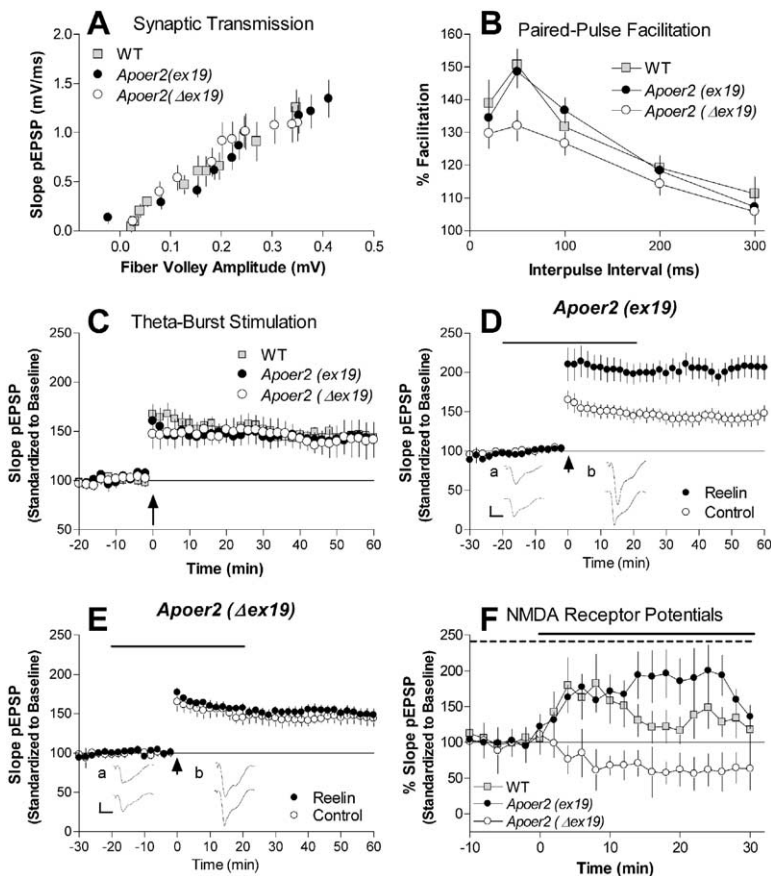
Figure 3. Reelin-Induced Activation of Long-Term Potentiation Requires Exon 19 of *Apoer2* and Modifies NMDA Receptor-Mediated Potentials

Synaptic transmission. (A) Synaptic transmission is presented as the slope of the field EPSP versus the fiber volley amplitude at increasing stimulus intensities for *Apoer2* (*ex19*) (●, n = 10), *Apoer2* (*Δex19*) (○, n = 15), and wild-type mice (□, n = 9).

Synaptic plasticity. (B) Short-term synaptic plasticity is evaluated by the amount of paired-pulse facilitation with interpulse intervals of 20, 50, 100, 200, and 300 ms [*Apoer2* (*ex19*) (●, n = 10), *Apoer2* (*Δex19*) (○, n = 15), and wild-type (□, n = 9).

(C) LTP induced with theta burst stimulation consisting of five trains of four pulses at 100 Hz with an interburst interval of 20 s. Normal LTP was induced in *Apoer2* (*ex19*) (●, n = 6) and *Apoer2* (*Δex19*) (○, n = 6) compared to wild-type mice (□, n = 9).

Reelin stimulation. (D and E) Hippocampal slices perfused with Reelin (●), compared to slices perfused with control media (○), in combination with theta burst stimulation caused a large increase in potentiation in *Apoer2* (*ex19*) ([D]; ●, n = 9; ○, n = 9), but no increase in potentiation was observed for *Apoer2* (*Δex19*) ([E]; ●, n = 9; ○, n = 8) (Reelin perfusion is represented with a black bar). (Insets) Representative pEPSP traces from Reelin perfusion experiments (mean of six successive EPSPs, mean ± SEM) (a) immediately before high-frequency stimulation (HFS) and (b) at 60 min post-tetanus obtained from Reelin (top traces) or control (bottom traces) perfusion experiments.

NMDA receptor-mediated potentials. (F) Slices were treated with CNQX (represented with a dotted line), and changes in field potentials mediated through NMDA receptors were determined for *Apoer2* (*ex19* ●, n = 10), *Apoer2* (*Δex19*) (○, n = 7), and wild-type mice (□, n = 6) following Reelin perfusion (represented with a black bar).

All data are presented as mean ± SEM.

Apoer2 ICD Influences Animal Behavior

Apoer2 is also necessary for normal associative learning using a fear conditioning test (Weeber et al., 2002). To better define the role of the alternatively spliced cytoplasmic insert in this learning paradigm, we assessed associative learning ability in wild-type and Apoer2 ICD mutants. We first performed two-trial fear conditioning by pairing an aversive stimulus (US; mild foot shock) with an acoustic component (CS; white noise) in a novel context. Fear response was assessed by the frequency at which normal motor behavior was disrupted by "freezing." The degree of freezing to the tone and shock during training was not significantly different between animal groups (data not shown). Figures 5A and 5B show the extent of short-term (1 hr, black bars) and long-term (24 hr, white bars) associative learning to the (acoustic) cue and the (environmental) context. The extent of learning was evaluated by the amount of freezing behavior of the animal.

Although both contextual and cued fear-conditioned learning are dependent on proper function of the amygdala, only the contextual component of fear-conditioned learning is hippocampus dependent. The cue test did not reveal any significant difference between the animal groups, although the *Apoer2* (*Δex19*) mice

showed a trend toward reduced freezing (Figure 5A). When compared to wild-type mice, the *Apoer2* (*ex19*) mutants (n = 11) showed comparable freezing to the reintroduction to the context (Figure 5B) at both 1 hr and 24 hr after training (p > 0.5, Dunnett's multiple comparison test). By contrast, the *Apoer2* (*Δex19*) (n = 11) mutant showed a highly significant reduction in freezing following the reintroduction to the context compared to wild-type mice (n = 19) (1 hr and 24 hr; $F_{[4, 45]} = 11.19$, p < 0.0001; one-way ANOVA) as well as compared to the *Apoer2* (*ex19*) mutant (p < 0.01, q = 4.5) at the 1 hr (p < 0.05) and 24 hr contextual test times (p < 0.01).

We also performed open-field, rotorod, prepulse inhibition, and hot plate tests to ensure that the observed deficits were not due to a pre-existing physical or behavioral deficit and found no significant differences in any of the animal groups compared to wild-type or to each other (data not shown). These observations indicate that both Apoer2 ICD mutants show overall normal activity, perception, motor coordination, and nociception, but that mutants that lack the alternatively spliced exon 19 show a severe contextual associative learning defect in the absence of auditory component deficits.

Our observations that hippocampus-dependent learning is impaired in the Apoer2 knockout (Weeber et al.,
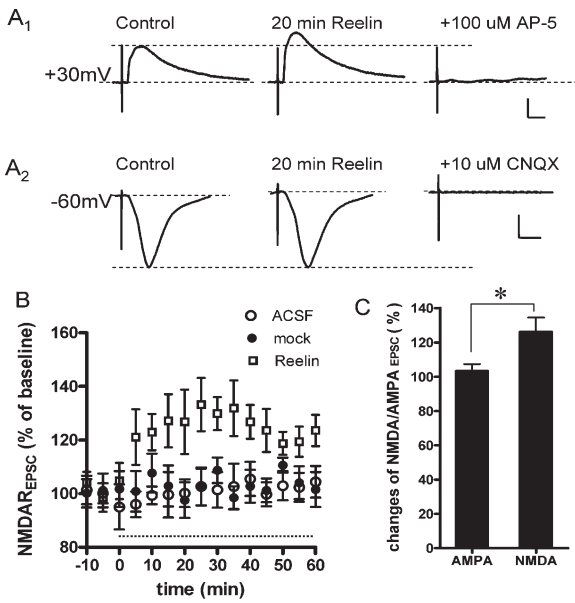
Figure 4. Reelin Selectively Increases Synaptic NMDAR-Mediated EPSCs in WT CA1 Pyramidal Neurons

(A) Slices were incubated in the absence or presence of Reelin (~5 nM) for 20 min prior to determination of NMDAR-mediated EPSCs, which were increased in response to Reelin application (A1), while AMPA EPSC were not affected (A2). AP-5 (100 μM) or CNQX (10 μM) was added at the end of each experiment to verify that the isolated EPSCs were NMDAR- and AMPAR-specific responses, respectively.

(B) Data were pooled (n = 7) to show the time course of Reelin effects on NMDA-EPSCs over a 1 hr period (indicated by the horizontal dotted line).

(C) Reelin affected primarily NMDAR-dependent EPSCs, while AMPA-EPSC were unchanged (103% ± 4% of control) following application of Reelin for 20 min in the presence of 100 μM AP-5. By contrast, NMDA-EPSC were markedly increased (126% ± 8% of control). *p < 0.05. n = 6.

Scale bar in (A1), 50 pA, 20 ms; (A2), 100 pA, 10 ms.

2002) and in the *Apoer2* (*Δex19*) mutant prompted us to determine if spatial learning might also be altered. Animal groups from all genotypes were trained in the Morris water maze task as described in Experimental Procedures. No significant differences were seen for *Apoer2* (*ex19*) (n = 14) or *Apoer2* (*Δex19*) (n = 15) mutants as compared to wild-type mice (n = 18) in the training portion of the hidden platform version of the Morris water maze (data not shown), and all groups showed a substantial improvement in their performance over the 11 days of the training period.

To determine if *Apoer2* ICD mutants were capable of learning to use spatial cues to locate the escape platform, we subjected them to a probe test on day 12. Animals from all groups employed a search strategy that focused on the quadrant in which the escape platform had been located. However, a significant effect of the genotype on the time spent in the target quadrant was observed (F[5, 155] = 6.92, p < 0.01, ANOVA). *Apoer2*−/− and *Apoer2* (*Δex19*) mutant mice showed reduced time in the training quadrant compared to wild-type mice (p < 0.01, Dunnett's multiple comparison
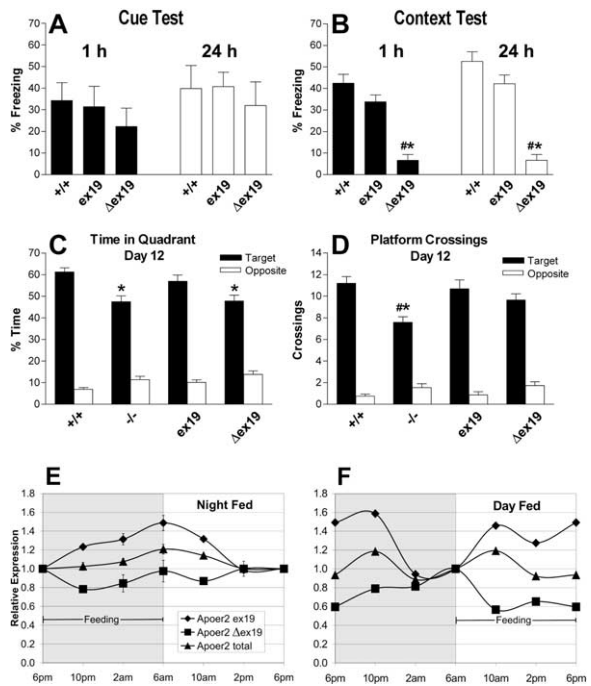

Figure 5. Normal Associative and Spatial Learning Requires Exon 19 of *Apoer2*

Fear conditioning/associative learning. Two-trial fear conditioning to assess associative learning 1 and 24 hr after two CS-US pairings. (A) No significant difference in the conditioned response was observed during the cue test between wild-type (n = 19) and mutant mice [*Apoer2* (*ex19*) (n = 11) and *Apoer2* (*Δex19*) (n = 11)] at either time point. (B) Assessment of freezing to the context revealed a conditioned response that was greater in both wild-type and *Apoer2* (*ex19*) (n = 11) mice compared to *Apoer2* (*Δex19*) (n = 11) at both times tested. *Morris water maze task/spatial learning.* Results from a probe trial on day 12 during a 60 s test time with the hidden platform removed. (C) Percentage of time spent in the target quadrant (black bar) and opposite quadrant (clear bar) is reduced in *Apoer2*−/− (n = 26) and *Apoer2* (*Δex19*) (n = 25) compared to wt (n = 33) and *Apoer2* (*ex19*) (n = 23). (D) The number of platform crossings during the probe test in the target quadrant (black bar) and opposite quadrant (clear bar) for wt (n = 33), *Apoer2*−/− (n = 26), *Apoer2* (*ex19*) (n = 23), and *Apoer2* (*Δex19*) (n = 25). (Mean ± SEM, number of n for training is consistent with probe trials; *p < 0.05 compared to wild-type mice; #p < 0.05 compared to *Apoer2* (*ex19*), Dunnett's multiple comparison test.) *Circadian regulation of alternative splicing of Apoer2 ex19.* (E and F) Relative mRNA expression of Apoer2 ex19 (♦), Apoer2 Δex19 (■), and total Apoer2 (▲). Mouse brain mRNA was isolated every 4 hr over a 24 hr period from night-fed (E) or day-fed (F) mice maintained on a normal light cycle. The shaded area indicates the dark cycle. Relative expression is normalized to the beginning of feeding period (bar), Apoer2 ex19 expression increases during the active period, while Apoer2 Δex19 decreases.

test). Consistent with the associative learning test, the *Apoer2* (*ex19*) mice thus learned to use spatial cues to form a better escape strategy compared to the *Apoer2*−/− and *Apoer2* (*Δex19*) mutants and were comparable to wild-type mice (Figure 5C). With respect to the number of platform crossings per quadrant, all animal groups demonstrated an overall trend in the probe test on day 12 (Figure 5D) that was similar to the quadrant test time when compared to the number of times

the mice passed over the identical platform area in the opposite quadrant ($F_{[5, 155]} = 7.77$, $p < 0.0001$, ANOVA). A significant decrease in the number of platform crossings was observed for $Apoer2^{-/-}$ mutants compared to wild-type ($p < 0.05$). This decrease did not reach significance in the $Apoer2$ ($\Delta ex19$) animals. As before, the $Apoer2$ ($ex19$) mice showed learning ability in the Morris water maze that was comparable to that of wild-type controls.

Taken together, these findings are consistent with the observed electrophysiological defects in hippocampal slices and suggest that the normal Reelin-induced tyrosine kinase signal is necessary for the modulation of synaptic plasticity that underlies hippocampus-dependent associative learning. The functional coupling of this signal appears to be disrupted in the ICD mutants that lack the alternatively spliced exon 19.

Alternative Splicing Is Modulated by Activity

To determine whether the splicing of the Apoer2 ICD is being modulated by behavioral or environmental factors, we analyzed the relative change of total Apoer2 mRNA, as well as the ex19 and $\Delta ex19$ isoforms, in the brains of wild-type mice over a 24 hr period by real-time PCR (Figure 5E). While the total amount of Apoer2 mRNA increased only slightly over the dark period in which mice normally feed and are most active, the ex19 mRNA species increased selectively during that time, accompanied by a concordant decrease of the $\Delta ex19$ isoform. During the period of reduced activity (light), the relative expression of ex19 mRNA decreased and $\Delta ex19$ levels rose. This shift in the relative abundance of either mRNA species was triggered by physical activity and not by the light cycle, since animals that were forced to feed solely during the day adjusted their splicing pattern to match the beginning of the feeding period, not the dark period (Figure 5F). Thus, selective splicing of ex19 mRNA occurs during the period of highest activity and declines during the resting phase.

Apoer2 Interacts with the NMDA Receptor and PSD-95

Glutamate receptors of the NMDA subtype are present in the postsynaptic density of excitatory synapses. NMDA receptor activation, like Apoer2, is necessary for long-term potentiation of synaptic strength (Malenka, 2003) and for hippocampus-dependent associative and spatial learning in mice. To investigate whether activation of Apoer2 and NMDA receptor might be functionally related, we tested whether Apoer2 can interact either directly or indirectly with NMDA receptor subunits and whether Apoer2 is also present in the synapse.

Cotransfection and coimmunoprecipitation with Apoer2, full-length NMDA receptor subunit 2A (NR2A), and anti-Apoer2 antibodies in 293 cells revealed that NR2A can indeed form a complex with Apoer2 (Figure 6A, lane 3). Similar results were obtained with the NR2B subunit of the NMDA receptor (data not shown). To determine, whether this interaction also occurs in vivo, we performed immunoprecipitation experiments from wild-type (Figure 6B, lane 1) and mutant (lanes 2–4) mouse brains. NR2A coprecipitated with Apoer2 from wild-type brain lysates (lane 1) and from both ICD mutant

strains (lanes 3 and 4), suggesting that the interaction of NR2A occurs either within the extracellular domains or through a motif in the cytoplasmic tail of Apoer2 that is common to all the ICD forms and that Apoer2 is physiologically present in NMDA receptor complexes in the CNS in vivo.

We have previously shown that PSD-95 can interact with the Apoer2 cytoplasmic domain through ex19-encoded sequences (Gotthardt et al., 2000). We confirmed this interaction by transfection experiments in 293 cells. FLAG-tagged Apoer2 constructs expressing the cytoplasmic tail containing (Figure 6C, lane 2) or not containing (lane 3) ex19 were cotransfected together with PSD-95 into 293 cells, and complexes were immunoprecipitated using an anti-FLAG antibody. Only the ex19-containing construct was able to mediate efficient PSD-95 binding and coprecipitation.

To obtain further evidence for the functional importance of the Apoer2 interaction with the NMDA receptor subunits, we immunoprecipitated the NR2A (Figure 6D) and NR2B (Figure 6E) subunits from hippocampal brain slices that had been incubated in the presence (solid bars) or absence (open bars) of Reelin in vitro. Immunoprecipitated proteins were then subjected to immunoblotting with an anti-phosphotyrosine antibody, and the amount of the phosphorylated protein was normalized to the total amount of NR2A or NR2B that was present in the precipitate. Tyrosine phosphorylation of NR2A and NR2B subunits was significantly increased in $Apoer2$ ($ex19$) slices in response to Reelin, but not in $Apoer2^{-/-}$ or Apoer2 ($\Delta ex19$) slices. These findings suggest that the Reelin signal acts on NMDA receptors that are present in a complex with Apoer2. This interaction, combined with activation of the Reelin signal, alters the functional properties of the NMDA receptor by a mechanism that is dependent upon the presence of Apoer2 exon 19 and that involves tyrosine phosphorylation of the NMDA receptor intracellular domains. PSD-95 may be involved in the ex19-dependent coupling of the signal, but not necessarily for the physical association of Apoer2 with the NMDA receptor complex.

Apoer2 Is Present in the Postsynaptic Density of Synapses

To determine whether the Reelin signaling complex is present in synapses in vivo where Apoer2 can topologically associate with the NMDA receptor, we investigated whether Apoer2 and Dab1 are present in the same synaptic subcompartment as the NMDA receptor, i.e., the postsynaptic density. We first prepared synaptosomes (Figure 7A, lane 2) from rat brain membrane fractions (lane 1) and separated them into a detergent-resistant postsynaptic density-containing fraction (lane 3) and a detergent-soluble fraction that contains presynaptic proteins (lane 4). Immunoblotting revealed the presence of Apoer2, Dab1, PSD-95, and NR2A exclusively in the postsynaptic density fraction. Synaptophysin, a presynaptic vesicle protein, was present exclusively in the detergent-soluble fraction.

To further support this biochemical finding, we next used cultured hippocampal neurons to localize Apoer2 and PSD-95 by immunocytochemistry (Figures 7B–7G).
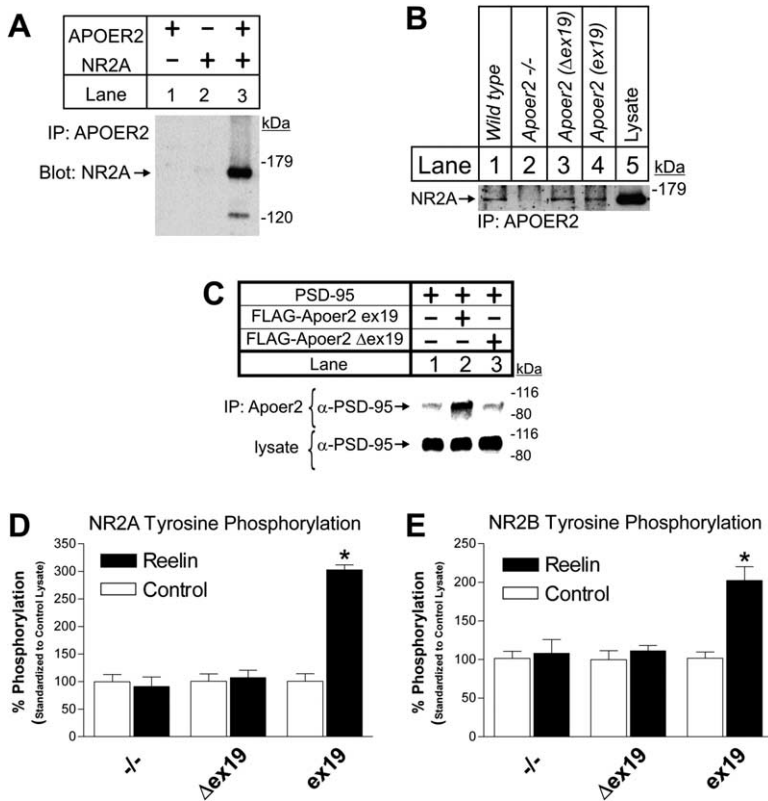
Figure 6. Apoer2 Associates with NMDA Receptor Subunits and with PSD-95

(A) Apoer2 directly associates with NR2A. HEK293 cells were transfected with the indicated expression vectors. Cell lysates were immunoprecipitated with an antibody directed against the Apoer2 carboxyl terminus, and precipitated proteins were immunoblotted with an antibody directed against NR2A. NR2A efficiently coprecipitates with Apoer2 (lane 3). Similar results were obtained with NR2B (data not shown).

(B) NR2A coprecipitates with Apoer2 from mouse brain lysates. Brain membranes were prepared from mice of the indicated genotype, and lysates (lane 5) were subjected to immunoprecipitation with an anti-Apoer2 antibody (αCT) as described in Experimental Procedures. NR2A was precipitated from wild-type (lane 1) and each of the ICD mutants (lanes 3 and 4), but not from the Apoer2 knockout (lane 2).

(C) Coimmunoprecipitation of PSD-95 with FLAG-tagged Apoer2 intracellular domains containing (lane 2) and not containing (lane 3) the ex19-encoded sequences; lane 1, negative control.

(D and E) Tyrosine phosphorylation of NR2A and NR2B subunits in response to Reelin. Mouse hippocampal brain slices from Apoer2$^{-/-}$, Apoer2 (Δex19), and Apoer2 (ex19) were incubated in the presence (filled bars) or absence (open bars) of recombinant Reelin. After detergent solubilization, NR2A and NR2B were immunoprecipitated and analyzed by immunoblotting with an anti-phosphotyrosine antibody. Error bars: SEM, p < 0.05.

Apoer2 (Figures 7B and 7E) was abundantly present on neuritic processes in a typical punctate synaptic staining pattern that overlapped (Merge, Figures 7D and 7G) with PSD-95 (Figures 7C and 7F), consistent with expression of Apoer2 in the postsynaptic densities of a subset of synapses.

To finally and conclusively demonstrate that Apoer2 is present in postsynaptic densities of hippocampal synapses in vivo, we performed immunoelectron-microscopy with affinity purified antibodies directed against Apoer2 in the hippocampus of mice expressing (Figure 7H) or lacking (Figure 7I) the alternatively spliced cytoplasmic exon. Both panels show the presence of immunogold-labeled IgG bound to Apoer2 within the postsynaptic density of two representative synapses in the CA1 region. Similar labeling was observed in wild-type sections (data not shown). To determine whether Apoer2 was expressed and distributed equally throughout the hippocampus of wild-type, ex19, and Δex19 animals, a total of 2400 synapses was assessed for Apoer2 expression by immunoelectron-microscopy in a minimum of three independent brains/genotype. Labeling was observed in 8.1%, 6.4%, and 8.3%, respectively, of all synapses throughout the CA1 region, indicating that the presence or absence of the alternatively spliced exon does not alter the synaptic expression or distribution of the receptor. These relative numbers of labeled synapses in the different mouse brains can only represent the lower limit of the total

number of synapses expressing Apoer2 in the hippo-campus and should not be interpreted in absolute terms. This is due to factors that influence the limits of detection, such as the relative abundance of Apoer2 and preservation of antibody epitopes during the fixation process.

Discussion

We have used a homologous knockin gene replacement approach to selectively express nonspliceable isoforms of the neuronal ApoE and Reelin receptor Apoer2 in the embryonic and adult mouse brain. The mutant mice exclusively express either one of two alternative splice forms of the cytoplasmic domain, containing or missing an inserted sequence of 59 amino acids (exon 19) (Figure 1). Mice lacking this alternatively spliced exon 19 are deficient in learning and memory tasks. This same exon is required for the modulation of LTP, NMDA receptor phosphorylation, and synaptic plasticity by Reelin. The Reelin signaling complex including Apoer2 is present in the synapse where it associates with NMDA receptors and the postsynaptic density protein, PSD-95. These findings reveal a role for Reelin and Apoer2 in the mammalian brain and establish a mechanism by which ApoE receptors modulate synapse function.

Impaired Reelin signaling in Apoer2 knockout mice results in abnormal cortical lamination and neuronal po-
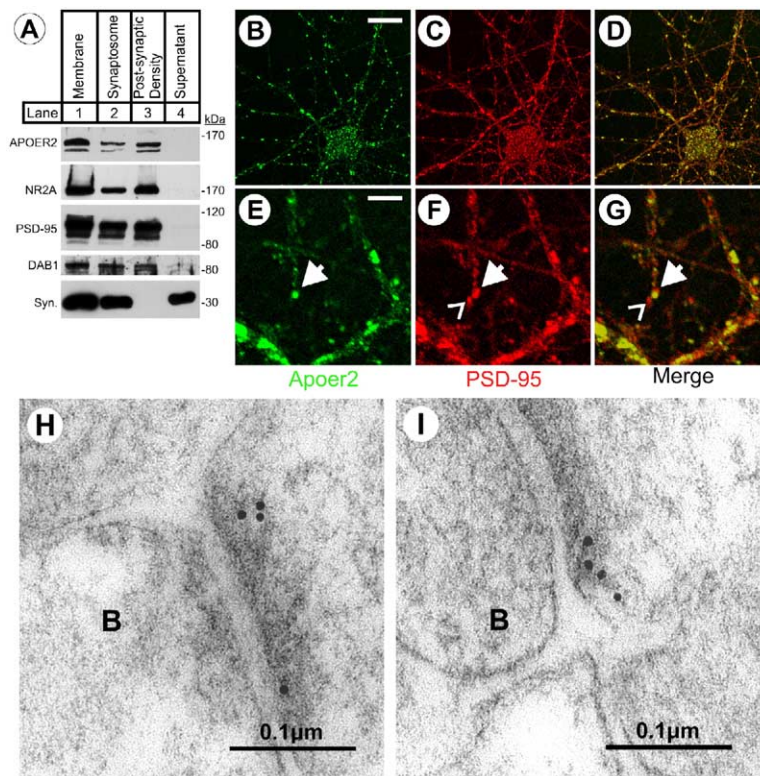
Figure 7. Apoer2 and Dab1 Are Present in the Postsynaptic Density

(A) Immunoblot analysis of Apoer2, NR2A, PSD-95, Dab1, and synaptophysin in rat brain membranes, synaptosomes, and post-synaptic and presynaptic fractions. Apoer2, NR2A, and PSD-95 are found exclusively in the postsynaptic density fraction; synapto-physin is present only in the detergent-solu-ble presynaptic fraction. Dab1 is found pre-dominantly in the postsynaptic fraction.
(B–G) Confocal microscopy of cultured pri-mary rat neurons. Apoer2 (B and E) was de-tected using affinity-purified antibodies and was found to colocalize with PSD-95 (C and F); (D) and (G) show the merged image. The arrow in (E)–(G) points to a synapse contain-ing Apoer2 and PSD-95. The arrowhead in (F) and (G) indicates a PSD-95-containing subcellular compartment that does not con-tain Apoer2. Scale bar = 20 μm (B–D); 5 μm (E–G).
(H and I) Immunoelectron microscopy of mouse brain reveals Apoer2 in the postsyn-aptic density in the stratum radiatum CA1 subregion of the hippocampus from Apoer2 ex19 (H) and Apoer2 Δex19 (I). Immunogold particles = 10 nm. Scale bar = 100 nm. B, synaptic bouton.

sitioning in the neocortex and hippocampus (Tromms-dorff et al., 1999), learning disabilities, and degradation of hippocampal LTP (Weeber et al., 2002). At the end of the neuronal migration period, the predominant embry-onic pattern of Reelin expression by Cajal-Retzius neu-rons in the marginal zone diminishes and is replaced through tangential migration by a subset of GABAergic interneurons (Drakew et al., 1998; Pesold et al., 1998) that originate from the medial ganglionic eminence and that enter the cortex and the hippocampus. The Reelin protein that is produced by these cells has been found in the vicinity of synapses (Pesold et al., 1999), and re-duced Reelin levels have been associated with patients suffering from schizophrenia (Impagnatiello et al., 1998). Taken together, these findings suggest that Reelin has distinct and different functions in the developing and in the adult brain.

To gain a better understanding of the specific roles of Apoer2 in the embryonic as well as in the mature brain, we investigated the significance of the alternative splice forms of the Apoer2 ICD on signaling in vivo. Both forms of Apoer2 are equally effective in directing neuronal migration during development, and lamination is normal in both strains (Figure 2). However, *Apoer2* (*Δex19*) animals had marked fear-conditioning defects and learning disabilities (Figure 5), and moreover, hip-pocampal slices from these animals were completely unresponsive to Reelin in the LTP assay (Figure 3E). By contrast, *Apoer2* (*ex19*) slices robustly responded to Reelin (Figure 3D) and maintained enhanced LTP with-out any degradation for the entire duration of the assay. The response exceeded that seen in slices from wild-type control mice (Weeber et al., 2002), which physio-logically express the *ex19* as well as the unresponsive *Δex19* ICD isoform. Together, these findings reveal that the modulatory role of Reelin in the adult brain is regu-lated by alternative splicing of the Apoer2, an event that is not required for normal neuronal migration. Rather, alternative splicing of the Apoer2 ICD was found to cor-relate with the feeding period during which the mice are awake and thus most actively process environmental sensory input. An intriguing speculation resulting from these findings is that Reelin signaling may actively pro-mote memory formation during the waking period and that this pathway appears to be reduced during resting periods when the animals sleep. This may have implica-tions for our understanding of the pathophysiology of schizophrenia, where Reelin expression has been found to be reduced.

NMDA receptors constitute a class of ionotropic postsynaptic glutamate receptors that are of funda-mental importance for learning, associative recall, and LTP expression, induction, and maintenance (Naka-zawa et al., 2002, 2003; Sheng and Kim, 2002; Tsien et al., 1996). Furthermore, Src family tyrosine kinases, which are activated by Reelin signaling, are essential for LTP expression. Among them, Fyn is of particular importance both for LTP (Grant et al., 1992) as well as for Reelin signaling (Arnaud et al., 2003; Bock and Herz, 2003), and tyrosine phosphorylation of NMDA receptor subunits contributes to the maintenance of LTP (Rostas et al., 1996).

Our findings show that Apoer2 and NMDA receptors are indeed physically and functionally coupled in vivo.
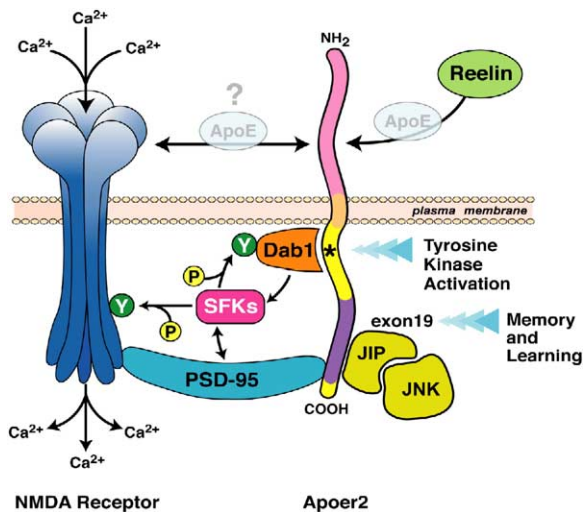
Figure 8. Hypothetical Model for NMDA Receptor Interaction with the Reelin Receptor Complex

Apoer2 is part of NMDA receptor complexes. PSD-95 may bind to the cytoplasmic domains of Apoer2 and NMDA receptors and promote the recruitment of Src family tyrosine kinases (SFK) into the complex, thereby facilitating interaction with and phosphorylation of Dab1. Binding of Reelin to Apoer2 leads to clustering of Apoer2, Dab1, and NMDA receptors, stimulation of SFK activity (Arnaud et al., 2003; Bock and Herz, 2003; Jossin et al., 2004; Strasser et al., 2004), and NMDA receptor phosphorylation (Figures 6D and 6E). This would result in increased Ca^{2+} conductance and increased potentiation. JNK recruitment through JIPs may further modulate synaptic response. ApoE has been shown to prevent Reelin binding to Apoer2 (Brandes et al., 2001; D'Arcangelo et al., 1999). Whether ApoE can also interfere with NMDA receptor interaction and to what extent this occurs in the synapse is currently unknown. Further refinement of this model will require the identification and selective mutation of the PSD-95 and JIP interaction sites within the ex19-encoded insert.

This is based on several independent lines of evidence: (1) Apoer2 isoforms selectively regulate NMDA, but not AMPA receptor activity as determined by field and single-cell measurements, (2) NMDA receptor subunits are present in complexes with Apoer2 (Figure 6), (3) Reelin induces tyrosine phosphorylation of NR2A and NR2B in hippocampal slice preparations in an Apoer2 isoform-specific manner (Figures 6D and 6E), (4) Apoer2 and Dab1 are present in the postsynaptic density fraction (Figure 7A), and (5) the alternatively spliced exon does not affect the synaptic distribution of the receptor. Taken together, these results support a model (Figure 8) in which the association of Apoer2 with NMDA receptors facilitates NMDA receptor tyrosine phosphorylation and conductance in response to Reelin. This model is further supported by independent evidence that Reelin potentiates calcium influx through NMDA receptors in cultured primary cortical neurons by a mechanism that is dependent on Dab1, Apoer2, and SFKs (Y. Chen, U.B., T.S. Tang, I. Bezprozvanny, and J.H., unpublished data).

What are the molecular interactions by which the insert encoded by exon 19 affects LTP? We currently know of two classes of interacting proteins that bind to epitopes within the insert: the c-Jun N-terminal kinase interacting proteins JIP1 and JIP2, and the PDZ domain containing protein PSD-95. Either protein alone or in combination may exert its biological effect by a different mechanism. JIPs serve as scaffolding proteins for a kinase cascade that activates JNK, a serine/threonine kinase that can modulate LTP (Curran et al., 2003). They have also been shown to bind to the motor protein kinesin (Verhey et al., 2001). PSD-95, on the other hand, binds to NMDA receptors and may serve in the recruitment of Src family kinases to the complex (Tezuka et al., 1999), which in turn might be required to properly present the cytoplasmic domains of the NMDA receptor subunits to the active kinase for phosphorylation (Figure 8). Our biochemical interaction and subcellular fractionation experiments, together with the light and immunoelectronmicroscopy results, suggest that Reelin signaling through Apoer2 modulates synaptic function mainly through a postsynaptic mechanism that involves tyrosine kinase activation.

One of the major mechanisms by which neurons control synaptic transmission is through spatial and temporal control of alternative splicing. The propagation of action potentials among neurons also requires the tuning of many different types of proteins, such as ion channels. Alternative splicing of the NR1 subunit of the NMDA receptor regulates trafficking of the receptor to the synapse and numerous protein-protein interactions that control essential physiological functions in the brain (Carroll and Zukin, 2002; Wenthold et al., 2003). NMDARs are heteromeric complexes of NR1 and NR2 subunits; therefore, the splicing of one subunit of the receptor complex can directly affect its regional and developmental expression. This regulation partly underlies the vast diversity and functionality of synapses in the brain. Here we have shown that different splice forms of Apoer2 can further modulate NMDA receptor functions and that Reelin, a novel signaling molecule that is secreted by a subset of GABAergic interneurons, can thereby modulate the properties of excitatory synapses. The properties of Reelin are different from those of rapidly acting neurotransmitters and rather resemble those of a locally acting neuropeptide that can adjust the gain or balance with which certain synapses react to excitatory input. The strength of this modulatory signal input in turn can also be adjusted by the receiving neurons through alternative splicing of Apoer2. ApoE, another ligand for Apoer2 and a major isoform-specific modifier of late-onset Alzheimer's disease, could in principle alter Apoer2 signaling and NMDAR response by interfering with normal receptor activation (Figure 8). Such a mechanism might contribute to the role of ApoE in Alzheimer's disease.

The biochemical and genetic evidence we have presented here expands the physiological functions of the developmental signaling pathway by which Reelin and ApoE receptors control the architecture of the brain to include a formerly unrecognized essential role in the regulation of neurotransmission in the synapses of the adult nervous system. Our findings have revealed a splice variant-dependent mechanism by which signals transmitted through LDL receptor family members di-

rectly modulate synaptic function, learning, and memory in the adult brain.

Experimental Procedures

Targeted Insertion of *Apoer2* Intracellular Domains
Site-directed mutagenesis (Stratagene, La Jolla, CA) was performed on a 434 bp *Apoer2* cDNA fragment including exons 17–20. Wild-type or mutant cDNA fragments were inserted into a genomic fragment including *Apoer2* exons 9–16, followed by a bovine growth hormone (BGH) polyadenylation signal. The modified genomic sequence was cloned into a plasmid containing a neomycin (*neo*) resistance gene expression cassette flanked by *loxP* sites. 129/SvJ embryonic stem (ES) cells (SM-1) were electroporated with SalI linearized targeting construct following standard protocols. *Neo*-resistant ES cell clones were isolated and analyzed for homologous recombination. ES cell clones were screened by a PCR strategy in which a 1 kb fragment including part of the *neo* cassette and exon 19 outside of the targeting region was amplified. Positively targeted ES cell clones were verified by Southern blot analysis, and the presence of the mutated ICD was confirmed by sequence analysis. Homologous recombination occurred in 1%–3% of all G418-resistant ES cell colonies in each of the constructs. We microinjected ES cell clones into C57BL/6J blastocysts and backcrossed male chimeras to C57BL/6J females for germ-line transmission. Since the *neo* cassette had the potential to affect the phenotype of knockin mice, we excised the floxed *neo* cassette in vivo by mating heterozygous mutant males with CAG-Cre transgenic females (Sakai and Miyazaki, 1997). We monitored excision of the *neo* cassette by using DNA digested with BglII and Southern blot analysis using an *Apoer2*-specific probe as well as Apoer2, Cre, and *neo* PCR genotyping. Primers used for cloning and genotyping can be supplied upon request.

Brain Histopathology
Sublethally anesthetized mice were perfused through the left ventricle with phosphate-buffered saline (PBS) followed by 4% paraformaldehyde in PBS. Dissected brains were postfixed by immersion in 4% paraformaldehyde for 16 hr and embedded in paraffin. 5 μm sagittal sections were stained with hematoxylin and eosin for histological analysis (at least three samples per genotype).

In Vitro Assay of Reelin Signaling
Primary cortical neurons were prepared from embryonic mouse brains and treated with Reelin or control-conditioned medium for 20 min as previously described (Beffert et al., 2002). Cell lysates were separated on SDS-PAGE gels, transferred to nitrocellulose, and blotted for proteins affected by Reelin signaling, including Dab1, phospho-(Ser473)-Akt, and Akt.

Hippocampal Slice Preparation and CA1 Electrophysiology
All protocols involving the use of animals for the following experiments were in compliance with the National Institutes of Health's Guide for the Care and Use of Laboratory Animals and the Baylor College of Medicine Institutional Animal Care and Use Committee. Hippocampal slice preparations and LTP measurements were performed on 3-month-old mice essentially as previously described (Weeber et al., 2002). Data from LTP experiments were analyzed using a two-way ANOVA, with post hoc tests performed using Dunnett's multiple comparisons test.

Synaptically evoked whole-cell responses of isolated NMDAR- or AMPAR-mediated EPSCs (NMDA-EPSC) of CA1 pyramidal neurons were obtained using an EPC10 double amplifier (Heka Elektronik) with the aid of DIC microscopy (Leica DMLSFA). Hippocampal slices were cut between the CA3 and CA1 region to prevent epileptiform activity and were preincubated for 30 min with 100 μM picrotoxin and additional 10 μM CNQX (NMDA-EPSC) or 100 μM AP-5 (AMPA-EPSC). The patch electrodes (4–7 MΩ) were filled with a solution containing 117 mM Cs gluconate, 10 mM tetraethylammonium-Cl, 10 mM HEPES, 8 mM NaCl, 5 mM QX314-Cl, 4 mM Mg^{2+}-ATP, 2.5 mM CsCl, 0.3 mM Na3GTP, and 0.2 mM EGTA and adjusted to pH 7.2, 280–290 mOsm. Neurons were held at +30 mV or −60 mV in whole-cell configuration, and series resistance (5–20 MΩ) was monitored throughout the experiment. Stimulus was driven by a Master-8-cp stimulator (A.M.P.I.) and delivered through a bipolar tungsten electrode (Frederick Haer) to Schaffer collateral fibers. Electric signals were digitized at 10 kHz and filtered at 2 kHz, stored on a PC computer, and analyzed offline using PatchMaster and Igor Pro software.

Mouse Behavior
Fear-conditioning experiments were carried out essentially as described in Weeber et al. (2002). A detailed description of the procedures relating to the fear conditioning and Morris Water maze experiments are provided in the Supplemental Data.

Quantitative Real-Time PCR
C57BL/6 mice were fed over a 2 week period only during the night (6 pm to 6 am) or only during the day (6 am to 6 pm) on a constant regular light cycle (light: 6 am to 6 pm). Total RNA was prepared from a pool of six brains at the indicated time of day by using an RNA STAT-60 Kit (Tel-Test, Friendswood, TX) and treated with DNase I (DNA-free; Ambion). First-strand cDNA was synthesized with random hexamer primers by using the ABI cDNA Synthesis Kit (Applied Biosystems), 2X SYBR Green PCR Master Mix (Applied Biosystems), and forward and reverse primers specific for mouse Apoer2 were added and real-time PCR quantification using the ABI PRISM 7900HT Sequence Detection System (Applied Biosystems) was performed. The following primer sequences were used for total Apoer2 (5′-AGTGTCCCGATGGCTCTGAC-3′, 5′-CAGCTTAACTTC TCGGCAGGA-3′), Apoer2 ex19 (5′-GCCCTCAAGGAGCTTTTT GTC-3′, 5′-AGGGTTCTTCGGGAGTTGGT-3′) and Apoer2 Δex19 (5′-CAGTGTACAGGAAAACGACAGAAGA-3′, 5′-TGCCACTCGTGC GGG-3′). All reactions were performed in triplicate. Relative amounts of mRNAs were calculated by using the comparative C_T method. As the invariant control, we used mouse cyclophilin mRNA.

Interactions and GST-Pulldowns
Apoer2 (full length, CAC38356; 870 amino acids) was expressed using pcDNA3.1 (Invitrogen). Apoer2 fragments containing the intracellular domain and without exon 19 were expressed in p3XFLAG-CMV-9 (Sigma). All transient transfections were carried out in HEK293 cells using FuGENE transfection reagent (Roche, Indianapolis, IN).

Brain Fractionation
Whole rat brains were dissected and homogenized in buffer A (50 mM Tris, pH 7.4, 2 mM $CaCl_2$) and 10% sucrose with a glass-Teflon homogenizer. The homogenate was centrifuged at 800 × g for 20 min and then again at 16,000 × g for 30 min. The resulting pellet was resuspended in 20 mM HEPES, 2 mM $CaCl_2$, pH 7.4, and centrifuged at 16,000 × g for 20 min. The pellet was resuspended in five volumes of 5 mM Tris-acetate, pH 8.1, 2 mM $CaCl_2$ for 45 min, sucrose was added to 35% w/vol and the sample was layered under equal volumes of 35%, 20%, and 10% sucrose in buffer A and centrifuged at 60,000 × g at 4°C for 2 hr. The distinct white synaptosomal layer is concentrated at the 10%–20% interface. The postsynaptic density (PSD) fraction was isolated by adding 1% Triton X-100 to the synaptosomal fraction, incubation for 30 min on ice, and centrifugation at 14,000 × g for 30 min.

NMDA Receptor Phosphorylation
Wild-type mouse hippocampal slices were cut on a vibratome as described above and incubated with control or Reelin containing medium for 25 min in perfusion buffer. Slices were then spun down, resuspended, and lysed in RIPA buffer and processed for immunoprecipitation with NR2A and NR2B antibodies.

Confocal Microscopy
For indirect immunofluorescence labeling, 2- to 3-week-old primary rat hippocampal neurons plated on coverslips in a glial coculture system were fixed in situ for 5 min with absolute methanol at −20°C. Slides were blocked with 1% BSA and 10% normal goat

serum in Tris-buffered saline, pH 9.0 (TBS). Neurons were incubated with affinity-purified antibodies directed against Apoer2 (αCT) or PSD-95 (Upstate Biotechnology, Waltham, MA) in blocking buffer overnight at 4°C, washed in TBS, and incubated with species-specific goat secondary antibodies coupled to Alexa Fluor 488 or Alexa Fluor 546 (Molecular Probes). Analysis was performed using a Leica TCS SP confocal microscope.

Electron Microscopy
Adult Apoer2 ICD mutant mice were deeply anesthetized with an overdose of Narkodorm-n (250 mg/kg body weight) and transcardially perfused with 0.9% saline followed by a fixative containing 4% paraformaldehyde, 0.1% glutaraldehyde, and 0.2% picric acid in 0.1 M phosphate buffer (pH 7.4). Brains were removed and postfixed in the same fixative overnight, cut on a vibratome into 300 μm sections, and the CA1 area of the hippocampus excised. Tissue blocks were cryoprotected in glycerol, cryofixed in nitrogen-cooled propane, substituted in methanol containing 1.5% uranylacetate, and embedded in Lowicryl HM20 (Chemische Werke Lowi, Waldkraiburg, Germany). Ultrathin sections were processed for post-embedding immunohistochemistry with an affinity-purified antibody directed against the carboxyl terminus of Apoer2 (αCT). Bound IgG was detected with a 10 nm gold-coupled anti-rabbit antibody (1:20, British BioCell International, Cardiff, UK). Control sections lacking exposure to the affinity-purified IgG were included in the same incubation procedure. Documentation was on a Zeiss 109 electron microscope using Macophot Ort 25 film.

Supplemental Data
The Supplemental Data, including figures and Experimental Procedures, can be found online at http://www.neuron.org/cgi/content/full/47/4/567/DC1/.

References

Alcantara, S., Ruiz, M., D'Arcangelo, G., Ezan, F., de Lecea, L., Curran, T., Sotelo, C., and Soriano, E. (1998). Regional and cellular patterns of reelin mRNA expression in the forebrain of the developing and adult mouse. J. Neurosci. *18*, 7779–7799.

Arnaud, L., Ballif, B.A., Forster, E., and Cooper, J.A. (2003). Fyn tyrosine kinase is a critical regulator of disabled-1 during brain development. Curr. Biol. *13*, 9–17.

Beffert, U., Morfini, G., Bock, H.H., Reyna, H., Brady, S.T., and Herz, J. (2002). Reelin-mediated signaling locally regulates protein kinase B/Akt and glycogen synthase kinase 3beta. J. Biol. Chem. *277*, 49958–49964.

Black, D.L., and Grabowski, P.J. (2003). Alternative pre-mRNA splicing and neuronal function. Prog. Mol. Subcell. Biol. *31*, 187–216.

Bock, H.H., and Herz, J. (2003). Reelin activates SRC family tyrosine kinases in neurons. Curr. Biol. *13*, 18–26.

Bock, H.H., Jossin, Y., Liu, P., Forster, E., May, P., Goffinet, A.M., and Herz, J. (2003). PI3-Kinase interacts with the adaptor protein Dab1 in response to Reelin signaling and is required for normal cortical lamination. J. Biol. Chem. *278*, 38772–38779.

Brandes, C., Novak, S., Stockinger, W., Herz, J., Schneider, W.J., and Nimpf, J. (1997). Avian and murine LR8B and human apolipoprotein E receptor 2: differentially spliced products from corresponding genes. Genomics *42*, 185–191.

Brandes, C., Kahr, L., Stockinger, W., Hiesberger, T., Schneider, W.J., and Nimpf, J. (2001). Alternative splicing in the ligand binding domain of mouse ApoE receptor-2 produces receptor variants binding reelin but not alpha 2-macroglobulin. J. Biol. Chem. *276*, 22160–22169.

Carroll, R.C., and Zukin, R.S. (2002). NMDA-receptor trafficking and targeting: implications for synaptic transmission and plasticity. Trends Neurosci. *25*, 571–577.

Curran, B.P., Murray, H.J., and O'Connor, J.J. (2003). A role for c-Jun N-terminal kinase in the inhibition of long-term potentiation by interleukin-1beta and long-term depression in the rat dentate gyrus in vitro. Neuroscience *118*, 347–357.

D'Arcangelo, G., Homayouni, R., Keshvara, L., Rice, D.S., Sheldon, M., and Curran, T. (1999). Reelin is a ligand for lipoprotein receptors. Neuron *24*, 471–479.

Drakew, A., Frotscher, M., Deller, T., Ogawa, M., and Heimrich, B. (1998). Developmental distribution of a reeler gene-related antigen in the rat hippocampal formation visualized by CR-50 immunocytochemistry. Neuroscience *82*, 1079–1086.

Gotthardt, M., Trommsdorff, M., Nevitt, M.F., Shelton, J., Richardson, J.A., Stockinger, W., Nimpf, J., and Herz, J. (2000). Interactions of the low density lipoprotein receptor gene family with cytosolic adaptor and scaffold proteins suggest diverse biological functions in cellular communication and signal transduction. J. Biol. Chem. *275*, 25616–25624.

Grabowski, P.J., and Black, D.L. (2001). Alternative RNA splicing in the nervous system. Prog. Neurobiol. *65*, 289–308.

Grant, S.G., O'Dell, T.J., Karl, K.A., Stein, P.L., Soriano, P., and Kandel, E.R. (1992). Impaired long-term potentiation, spatial learning, and hippocampal development in fyn mutant mice. Science *258*, 1903–1910.

Hiesberger, T., Trommsdorff, M., Howell, B.W., Goffinet, A., Mumby, M.C., Cooper, J.A., and Herz, J. (1999). Direct binding of Reelin to VLDL receptor and ApoE receptor 2 induces tyrosine phosphorylation of disabled-1 and modulates tau phosphorylation. Neuron *24*, 481–489.

Howell, B.W., Herrick, T.M., and Cooper, J.A. (1999a). Reelin-induced tryosine phosphorylation of disabled 1 during neuronal positioning. Genes Dev. *13*, 643–648.

Howell, B.W., Lanier, L.M., Frank, R., Gertler, F.B., and Cooper, J.A. (1999b). The disabled 1 phosphotyrosine-binding domain binds to the internalization signals of transmembrane glycoproteins and to phospholipids. Mol. Cell. Biol. *19*, 5179–5188.

Howell, B.W., Herrick, T.M., Hildebrand, J.D., Zhang, Y., and Cooper, J.A. (2000). Dab1 tyrosine phosphorylation sites relay positional signals during mouse brain development. Curr. Biol. *10*, 877–885.

Impagnatiello, F., Guidotti, A.R., Pesold, C., Dwivedi, Y., Caruncho, H., Pisu, M.G., Uzunov, D.P., Smalheiser, N.R., Davis, J.M., Pandey, G.N., et al. (1998). A decrease of reelin expression as a putative vulnerability factor in schizophrenia. Proc. Natl. Acad. Sci. USA *95*, 15718–15723.

Jossin, Y., Ignatova, N., Hiesberger, T., Herz, J., Lambert de Rouvroit, C., and Goffinet, A.M. (2004). The central fragment of

Reelin, generated by proteolytic processing in vivo, is critical to its function during cortical plate development. J. Neurosci. *24*, 514–521.

Malenka, R.C. (2003). The long-term potential of LTP. Nat. Rev. Neurosci. *4*, 923–926.

Nakazawa, K., Quirk, M.C., Chitwood, R.A., Watanabe, M., Yeckel, M.F., Sun, L.D., Kato, A., Carr, C.A., Johnston, D., Wilson, M.A., and Tonegawa, S. (2002). Requirement for hippocampal CA3 NMDA receptors in associative memory recall. Science *297*, 211–218.

Nakazawa, K., Sun, L.D., Quirk, M.C., Rondi-Reig, L., Wilson, M.A., and Tonegawa, S. (2003). Hippocampal CA3 NMDA receptors are crucial for memory acquisition of one-time experience. Neuron *38*, 305–315.

Pesold, C., Impagnatiello, F., Pisu, M.G., Uzunov, D.P., Costa, E., Guidotti, A., and Caruncho, H.J. (1998). Reelin is preferentially expressed in neurons synthesizing gamma-aminobutyric acid in cortex and hippocampus of adult rats. Proc. Natl. Acad. Sci. USA *95*, 3221–3226.

Pesold, C., Liu, W.S., Guidotti, A., Costa, E., and Caruncho, H.J. (1999). Cortical bitufted, horizontal, and Martinotti cells preferentially express and secrete reelin into perineuronal nets, nonsynaptically modulating gene expression. Proc. Natl. Acad. Sci. USA *96*, 3217–3222.

Rostas, J.A., Brent, V.A., Voss, K., Errington, M.L., Bliss, T.V., and Gurd, J.W. (1996). Enhanced tyrosine phosphorylation of the 2B subunit of the N-methyl-D-aspartate receptor in long-term potentiation. Proc. Natl. Acad. Sci. USA *93*, 10452–10456.

Sakai, K., and Miyazaki, J. (1997). A transgenic mouse line that retains Cre recombinase activity in mature oocytes irrespective of the cre transgene transmission. Biochem. Biophys. Res. Commun. *237*, 318–324.

Sheng, M., and Kim, M.J. (2002). Postsynaptic signaling and plasticity mechanisms. Science *298*, 776–780.

Stockinger, W., Brandes, C., Fasching, D., Hermann, M., Gotthardt, M., Herz, J., Schneider, W.J., and Nimpf, J. (2000). The reelin receptor ApoER2 recruits JNK-interacting proteins-1 and -2. J. Biol. Chem. *275*, 25625–25632.

Stolt, P.C., Jeon, H., Song, H.K., Herz, J., Eck, M.J., and Blacklow, S.C. (2003). Origins of peptide selectivity and phosphoinositide binding revealed by structures of Disabled-1 PTB domain complexes. Structure (Camb) *11*, 569–579.

Strasser, V., Fasching, D., Hauser, C., Mayer, H., Bock, H.H., Hiesberger, T., Herz, J., Weeber, E.J., Sweatt, J.D., Pramatarova, A., et al. (2004). Receptor clustering is involved in reelin signaling. Mol. Cell. Biol. *24*, 1378–1386.

Strickland, D.K., Gonias, S.L., and Argraves, W.S. (2002). Diverse roles for the LDL receptor family. Trends Endocrinol. Metab. *13*, 66–74.

Tezuka, T., Umemori, H., Akiyama, T., Nakanishi, S., and Yamamoto, T. (1999). PSD-95 promotes Fyn-mediated tyrosine phosphorylation of the N-methyl-D-aspartate receptor subunit NR2A. Proc. Natl. Acad. Sci. USA *96*, 435–440.

Tissir, F., and Goffinet, A.M. (2003). Reelin and brain development. Nat. Rev. Neurosci. *4*, 496–505.

Trommsdorff, M., Borg, J.P., Margolis, B., and Herz, J. (1998). Interaction of cytosolic adaptor proteins with neuronal apolipoprotein E receptors and the amyloid precursor protein. J. Biol. Chem. *273*, 33556–33560.

Trommsdorff, M., Gotthardt, M., Hiesberger, T., Shelton, J., Stockinger, W., Nimpf, J., Hammer, R.E., Richardson, J.A., and Herz, J. (1999). Reeler/Disabled-like disruption of neuronal migration in knockout mice lacking the VLDL receptor and ApoE receptor 2. Cell *97*, 689–701.

Tsien, J.Z., Huerta, P.T., and Tonegawa, S. (1996). The essential role of hippocampal CA1 NMDA receptor-dependent synaptic plasticity in spatial memory. Cell *87*, 1327–1338.

Verhey, K.J., Meyer, D., Deehan, R., Blenis, J., Schnapp, B.J., Rapoport, T.A., and Margolis, B. (2001). Cargo of kinesin identified as JIP scaffolding proteins and associated signaling molecules. J. Cell Biol. *152*, 959–970.

Weeber, E.J., Beffert, U., Jones, C., Christian, J.M., Forster, E., Sweatt, J.D., and Herz, J. (2002). Reelin and ApoE receptors cooperate to enhance hippocampal synaptic plasticity and learning. J. Biol. Chem. *277*, 39944–39952.

Wenthold, R.J., Prybylowski, K., Standley, S., Sans, N., and Petralia, R.S. (2003). Trafficking of NMDA receptors. Annu. Rev. Pharmacol. Toxicol. *43*, 335–358.

Yun, M., Keshvara, L., Park, C.G., Zhang, Y.M., Dickerson, J.B., Zheng, J., Rock, C.O., Curran, T., and Park, H.W. (2003). Crystal structures of the Dab homology domains of mouse disabled 1 and 2. J. Biol. Chem. *278*, 36572–36581.